

Phase-plane analysis of driven multi-lane exclusion models

Vandana Yadav, Rajesh Singh and Sutapa Mukherji

Department of Physics, Indian Institute of Technology, Kanpur-208 016

(Dated: March 14, 2018)

We show how a fixed point based boundary-layer analysis technique can be used to obtain the steady-state particle density profiles of driven exclusion processes on two-lane systems with open boundaries. We have considered two distinct two-lane systems. In the first, particles hop on the lanes in one direction obeying exclusion principle and there is no exchange of particles between the lanes. The hopping on one lane is affected by the particle occupancies on the other, which thereby introduces an indirect interaction among the lanes. Through a phase plane analysis of the boundary layer equation, we show why the bulk density undergoes a sharp change as the interaction between the lanes is increased. The second system involves one lane with driven exclusion process and the other with biased diffusion of particles. In contrast to the previous model, here there is a direct interaction between the lanes due to particle exchange between them. In this model, we have looked at two possible scenarios with constant (flat) and non-constant bulk profiles. The fixed point based boundary layer method provides a new perspective on several aspects including those related to maximal/minimal current phases, possibilities of shocks under very restricted boundary conditions for the flat profile but over a wide range of boundary conditions for the non-constant profile.

I. INTRODUCTION

Many unique non-equilibrium phenomena such as boundary-induced phase transitions [1], spontaneous symmetry breaking [2], phase separation [3] are observed in one-dimensional driven exclusion processes. These features that are very special to systems far-from-equilibrium led to extensive studies of variety of driven processes. Major developments in this direction started with the asymmetric simple exclusion process (ASEP) in which particles, after being injected at one boundary at a specific rate, hop in a specific direction on a finite one-dimensional lattice obeying mutual exclusion rule [4, 5]. A steady particle current is sustained through withdrawal of particles from the other boundary at a given rate. This simple model was later followed by more general systems involving more than one species of particles [2, 6, 7], more complicated lattice [8–14] or dynamics of particles [15] etc. All these models have a few common, basic features such as hopping of particles with bias in one direction and hence a nonzero particle flux, mutual exclusion between the particles and open boundaries with particle injection and withdrawal at given rates. In contrast to equilibrium systems, these one-dimensional, driven, many particle systems exhibit boundary induced phase transitions in their steady-state. In various phases, density profiles have distinct shapes which, for a given process, are completely dependent on the boundary rates. The boundary rates, therefore, are the most natural variables for the phase-diagram representing the phases and phase transitions.

In order to characterize the phase transitions, it often appears convenient to look at the steady-state density profile which describes the average particle occupancy of various sites. Density profiles have interesting shapes with extended bulk parts and one or more boundary layer parts which are narrow regions over which the density varies rapidly. The nature and location of the bulk, as

well as the boundary layer parts of the profile, change as the boundary rates change. For example, the boundary layers may be located near one or both the boundaries or may appear in the interior of the lattice. The latter one, commonly known as a shock, separates high and low density bulk regions [16]. That the boundary layer need not be confined to the boundary alone and the formation of a shock can be well characterized through a deconfinement transition of the boundary layer from the boundary have been shown in [17–19]. In the next section, we shall provide a more technical description of the boundary layer in terms of an appropriate differential equation.

Recent studies [17–19] show that the information about the bulk density can be obtained by studying the boundary layer parts of the density profile. Although methods of boundary layer analysis [20] allow us to find the analytical expressions of the boundary layers [17], in many cases, it becomes technically challenging to obtain analytical expressions for the boundary layers. However, since the boundary layers are expected to merge to the bulk in the appropriate limit, one may obtain information about the bulk density by studying the fixed points of the differential equations describing the boundary layers. For constant bulk profiles, this method is especially powerful since, in this case, the bulk densities must be the same as the fixed point values of the boundary layer equation.

In the present work, we apply fixed point based boundary layer method [7] to two driven many-particle systems, each composed of two one-dimensional lattices or lanes. Every lane has N sites and particles can hop to the neighboring sites on the lane obeying specific rules that are mentioned in detail in the respective sections. The particle dynamics of the two models considered here differ due to the following reasons. In the first model, particles do not hop from one lane to the other but the hopping rate on one lane changes based on the particle occupancy of the neighboring sites on the other lane [8, 9, 14].

In contrast, the second model involves two lanes which can mutually exchange particles. While particles on one lane undergo asymmetric simple exclusion process with hopping in a specific direction, those on the other lane undergo biased diffusion [10, 12, 13]. Such driven systems have similarities with intracellular transport processes in which molecular motors, receiving energy from the hydrolysis of adenosine triphosphate (ATP), move in a particular direction along microtubules. The first model may mimic the situation where a molecular motor moving along one channel with a large cargo attached to it creates an obstruction for the motion of other molecular motors on the neighboring channel. A second lane with particle diffusion on it has been introduced earlier to represent the environment in which molecular motors diffuse during the period when they are not attached to the microtubule [10]. More recently, similar two-lane models have been introduced to describe extraction of membrane tubes by molecular motors [12, 13]. In both the models that we study here, lanes are coupled to boundary reservoirs that maintain specific densities at the two ends of a lane. Our primary aim is to illustrate how the method can be used to predict steady-state density profiles under different boundary conditions and to quantify various features of the boundary layers including the height of the shock, approach to the bulk etc.

The motivation behind this study stems from the fact that till now there exists no general framework to study phase transitions of this small class of non-equilibrium systems. Although this is a much bigger issue concerning the entire subject of non-equilibrium statistical mechanics, lack of a general framework even for these driven systems is surprising. Due to the presence of more than one density variable, driven multi-lane systems [8–14], in general, are technically challenging. Previous studies on two lane systems, with particle occupancy on one lane affecting the hopping on the other, show that this issue requires a generalization of the extremal current principle [14] which has been used earlier to predict the phase diagram of a single lane ASEP involving a single density variable [15, 21]. Inadequacy of mean-field analysis for certain cases has motivated development of cluster approximation [9] and all these studies have revealed existence of new interesting phases including symmetry breaking. Studying the stability properties of the bulk plateaux, a variety of phase diagrams has also been found for systems with ASEP on one lane coupled to different kinds of particle’s motion on the other lane [13]. All these observations motivate us to verify the versatility of the boundary layer based method to this class of problems. The present paper is restricted to only two specific models from this class. It would be interesting to apply this method to study phase diagrams of other variants of two lane systems. This will be discussed in our future publications.

The present method appears to be general since it does not rely on any explicit analytical solution of the density profile, yet it provides a lot of physical insight regard-

ing the location of the boundary layer, value of the bulk density, nature of the phase transitions etc; all these obtained analytically through a phase-plane analysis of the differential equation describing the boundary layer. We predict the shape of the entire density profile from the fixed points and the phase portraits of the boundary layer equation. Most importantly, we find that various known results, obtained through development of different methods and hypotheses including extremal current principle, follow as natural consequence of the phase-portrait of the boundary layer differential equation. There are resemblances between the present method and the extremal current principle but it would require more work to establish a direct connection which might provide a natural basis for the hypothesis made for the extremal current principle.

The stochastic dynamics of particles undergoing ASEP can be described through discrete master equations. For large N ($N \rightarrow \infty$), and small lattice spacing, a ($a \rightarrow 0$) with Na finite, we may go over to a continuum limit in which a lattice site i is replaced by a continuous position variable $x = i/N$. In the continuum, long time, long length scale limit (the so called hydrodynamic limit), a statistically averaged master equation appears like a continuity equation describing the time-evolution of a density variable, say, $\rho(x, t)$, in terms of the particle current j . Since bulk phase transitions are large length scale phenomena and only certain gross features are crucial at these length scales, a continuum formulation is expected to be sufficient for our purpose. Our boundary-layer method is applicable to the steady-state version of such continuum equation. It is important to note that this continuum approach, however, produces a narrow boundary layer whose width varies with N . This will be shown explicitly in the next section by obtaining the boundary-layer solution for the simplest ASEP model introduced at the beginning.

An explicit derivation of the steady-state hydrodynamic equation requires obtaining the stationary flux, $j(\rho)$ from the microscopic dynamics of the model. For the first model, this derivation is simple due to spatially uncorrelated nature of the steady-state [8] and for the second model, we use a mean-field current-density relation. Since our primary aim is to elucidate how the fixed point based boundary-layer method works, we have used mean-field approximation for convenience. It will be clear from the analysis that the method is robust in the sense that it works equally well for other hydrodynamic equations irrespective of the approximation that has been used to derive these. Hence, the outcome of this method is exact to the extent to which the starting hydrodynamic equation is exact. A phase-plane analysis for the first model shows that, for certain boundary conditions, the density profile is strongly influenced by a saddle fixed point of the boundary layer differential equation and finally, as a consequence of this, the bulk profile changes drastically to a new value as the interaction between the lanes is increased. The second model provides an interesting

fixed point diagram with saddle-node bifurcations of the fixed points [22] of the boundary layer equation. These bifurcations appear at special densities that correspond to the maximum or minimum of the particle current and maximal/minimal current phases appear as natural consequences of the flow trajectories towards these special densities.

In section II, we discuss a few general properties of the boundary layer solution. Section III presents the phase plane analysis of the first model. In section IV, we consider the second model with two distinct cases of constant and non-constant bulk profiles. We summarize our main findings in section V.

II. BOUNDARY LAYERS

In order to illustrate some of the basic features of the boundary layer, here we choose the simplest model of ASEP in which particles hop in a particular direction on one lane obeying the exclusion rule. In addition, we also include processes that involve adsorption and evaporation of particles to and from the lane at rates proportional to ω_a and ω_d , respectively. The lane is coupled to boundary reservoirs which maintain fixed particle densities, ρ_l and ρ_r , at left and right boundaries of the lane. For the following equation, equal particle adsorption and evaporation rates are assumed. In a continuum mean-field description with the lattice size scaled to unity ($Na = 1$), the density variable $\rho(x, t)$ satisfies the differential equation

$$\frac{\partial \rho}{\partial t} = \epsilon \frac{\partial^2 \rho}{\partial x^2} + (2\rho - 1) \frac{\partial \rho}{\partial x} + \Omega(1 - 2\rho). \quad (1)$$

Here $\Omega = \omega_a N = \omega_d N$ and $\epsilon = \frac{1}{2N}$ is a small parameter. In the absence of adsorption and evaporation processes, the hydrodynamic equation with only hopping of particles can be expressed in the form of a continuity equation $\frac{\partial \rho}{\partial t} = -\frac{\partial}{\partial x}(-\epsilon \frac{\partial \rho}{\partial x} + j_\rho)$, where $j_\rho = \rho(1 - \rho)$ is the particle current associated with the hopping process. In addition, there is a diffusive current which appears along with a prefactor, ϵ , which becomes small as $N \rightarrow \infty$. In order to obtain the steady-state density profile, we need to solve

$$\epsilon \frac{d^2 \rho}{dx^2} + (2\rho - 1) \frac{d\rho}{dx} + \Omega(1 - 2\rho) = 0 \quad (2)$$

with boundary conditions $\rho(x = 0) = \rho_l$ and $\rho(x = 1) = \rho_r$.

In the limiting case, $\epsilon = 0$, equation (2) becomes a first order equation and its solution cannot, in general, satisfy two boundary conditions. The vanishing higher-order derivative term, also known as the regularization term, helps avoiding the singularity in the differential equation. In these problems, boundary layers are expected to appear near either one of the boundaries or in the interior of the lane. Based on the values of the boundary densities, different solutions arise and the techniques

of the boundary-layer analysis allow one to obtain uniform approximation to the solution of (2) order by order in ϵ under given boundary conditions. For very small ϵ , the second order derivative term of equation (2) can be neglected. The solution of the resulting first order equation describes the major part of the density profile. This solution, known as the outer solution in the boundary-layer language, is referred in the following as the bulk solution. For this particular example, the bulk solution is

$$\rho_o(x) = \Omega x + C_0 \quad (3)$$

with C_0 being the integration constant whose value can be determined from the boundary condition that this solution satisfies. For example, for a density profile with the bulk part satisfying the boundary condition at $x = 0$, $C_0 = \rho_l$. It is possible that along with this bulk solution, a boundary layer appears near $x = 1$ (see figure 1 for a typical density profile that appears in the low density phase for the ASEP under consideration [16, 17]). The boundary layer here satisfies the boundary condition at $x = 1$ and merges to the bulk solution at the other end. In order to satisfy two conditions, the second derivative term of (2) becomes necessary for the description of the boundary layer. Thus, in general, higher order derivative terms dominate the behavior in the boundary layer. To focus on the boundary layer, we introduce a rescaled variable $\tilde{x} = \frac{x-x_0}{\epsilon}$, where x_0 , which is arbitrary at this stage, specifies the location of the boundary layer after appropriate boundary conditions are implemented. In terms of this rescaled variable, (2) appears as

$$\frac{d^2 \rho}{d\tilde{x}^2} + (2\rho - 1) \frac{d\rho}{d\tilde{x}} + \epsilon \Omega(1 - 2\rho) = 0. \quad (4)$$

The $O(\epsilon^0)$ solution of the boundary layer can be obtained from

$$\frac{d^2 \rho}{d\tilde{x}^2} + (2\rho - 1) \frac{d\rho}{d\tilde{x}} = 0. \quad (5)$$

Since, the boundary layer is narrow, this also implies that at this order, the particle non-conserving processes have negligible influence on the boundary layer. Irrespective of their appearance in the interior or the boundary of the lane, solution of such equations are, in general, referred as the boundary layer solutions in the following. If the boundary layer appears near $x = 1$, we expect the boundary layer solution to merge to the bulk at $\tilde{x} \rightarrow -\infty$ and satisfy the boundary condition $\rho(\tilde{x} = 0) = \rho_r$. For boundary layers appearing in the interior of a lane separating high and low density bulk solutions, we expect the boundary layer solution to merge to appropriate bulk densities in the $\tilde{x} \rightarrow \pm\infty$ limits.

Integrating (5) once, we have

$$\frac{d\rho}{d\tilde{x}} + (\rho^2 - \rho) = c_0, \quad (6)$$

where c_0 is the integration constant. The saturation of the boundary layer to the bulk density, $\rho_b = \rho_o(x = 1)$,

case. From now onwards, we use $m = 1 - \beta$. These equations are to be supplemented with the boundary conditions ($\rho(x = 0) = \rho_l$, $\rho(x = 1) = \rho_r$) and ($\sigma(x = 0) = \sigma_l$, $\sigma(x = 1) = \sigma_r$) at the two ends of the lanes. Instead of considering nonlinear regularization terms, we follow a phenomenological approach and choose simpler regularization terms of the form $\epsilon \frac{d^2 \rho}{dx^2}$ and $\epsilon \frac{d^2 \sigma}{dx^2}$. After studying the steady-state for this simpler situation, we argue that no new feature emerges with the actual regularization terms.

Hydrodynamic equations that we study in the following are,

$$-\frac{\partial j_\rho}{\partial x} + \epsilon \frac{\partial^2 \rho}{\partial x^2} = 0 \text{ and} \quad (11)$$

$$-\frac{\partial j_\sigma}{\partial x} + \epsilon \frac{\partial^2 \sigma}{\partial x^2} = 0. \quad (12)$$

Equations (11) and (12) admit constant solutions which correspond to constant bulk profiles. For the boundary-layer solutions, we re-express these equations in terms of \tilde{x} and integrate once to obtain

$$\frac{\partial \rho}{\partial \tilde{x}} = \rho(1 - \rho)(1 - m\sigma) + c_1, \quad (13)$$

$$\frac{\partial \sigma}{\partial \tilde{x}} = \sigma(1 - \sigma)(1 - m\rho) + d_1. \quad (14)$$

Here c_1 and d_1 are the two integration constants. The saturation of the boundary layers to the bulk densities ρ_b and σ_b is ensured through the choice

$$c_1 = -\rho_b(1 - \rho_b)(1 - m\sigma_b), \text{ and} \quad (15)$$

$$d_1 = -\sigma_b(1 - \sigma_b)(1 - m\rho_b). \quad (16)$$

To begin with, we consider a situation where a density profile has a constant bulk part satisfying one boundary condition and a boundary-layer part satisfying the other boundary condition. As discussed earlier, one may conclude that the bulk density value which is also a boundary density at one end, is a fixed point of the boundary layer equation. The boundary layer, in this case, is the solution of (13) and (14) that starts from an initial density, which, here, is the boundary condition satisfied by the boundary layer, and approaches the fixed point.

Hence, for a set of boundary conditions, we may find out all the fixed points of the boundary layer equations with c_1 and d_1 fixed by assuming bulk densities to be same as one set of the boundary values. Whether this choice of bulk density and the corresponding boundary layer form an acceptable solution for the density profile, depends on the stability properties of fixed points and the phase-plane trajectories. Although settling this issue is much simple when the boundary layer equation has only stable or unstable fixed points, this is not so when the boundary layer equation has a saddle fixed point in addition to stable or unstable fixed points. In order to see these features, the most general approach would be to obtain the fixed point diagram as functions c_1 and d_1 . For finding out the fixed points, ρ^* and σ^* , one has to solve algebraic equations, $\rho^*(1 - \rho^*)(1 - m\sigma^*) + c_1 = 0$ and $\sigma^*(1 - \sigma^*)(1 - m\rho^*) + d_1 = 0$. Solving a fifth order polynomial equation for either ρ^* or σ^* , one may find five fixed points of which only real, positive fixed points of values ρ^* (and σ^*) ≤ 1 are the physically acceptable ones. Clearly, this would require a multi-dimensional parameter space on which the topology of the manifolds describing the fixed-point would be displayed. Instead of this detailed fixed point diagram, one may also find fixed points of (13) and (14) with values of c_1 and d_1 obtained for all possible combinations of ρ_b and σ_b . This allows us to have a generic picture for the number of physically acceptable fixed-points and their stability properties on the entire $\rho_b - \sigma_b$ plane.

Instead of providing a detailed picture, we consider a specific case of bulk densities $\rho_b = 0.4$, and $\sigma_b = 0.01$. It turns out that this corresponds to the same shape of the density profile we have just discussed. Out of five sets of fixed points of the boundary layer equation, only two sets are physically meaningful and these fixed points govern the phase-plane trajectories of the boundary layer solutions. The other fixed points are not crucial for our analysis since these are either imaginary or are unphysical (fixed point values larger than 1). Table 1, in the following, provides a list of values of c_1 , d_1 , two physically acceptable sets of fixed points (ρ_1^*, σ_1^*) and (ρ_2^*, σ_2^*), and the corresponding sets of eigenvalues ($\lambda_{11}, \lambda_{12}$) and ($\lambda_{21}, \lambda_{22}$) for different values of m .

| m | c_1 | d_1 | (ρ_1^*, σ_1^*) | (ρ_2^*, σ_2^*) | $(\lambda_{11}, \lambda_{12})$ | $(\lambda_{21}, \lambda_{22})$ |
|------|-----------|------------|--------------------------|--------------------------|--------------------------------|--------------------------------|
| 0.48 | -0.23884 | -0.00799 | (0.4,0.01) | (0.5992,0.01134) | (0.7927,0.1981) | ((0.698,-0.199) |
| 0.51 | -0.23877 | -0.00788 | (0.4,0.01) | (0.5991,0.0114) | (0.781,0.198) | (0.6808,-0.1997) |
| 0.58 | -0.238608 | -0.00760 | (0.4,0.01) | (0.598, 0.01178) | (0.754,0.197) | (0.638,-0.195) |
| 0.68 | -0.238368 | -0.0072072 | (0.4,0.01) | (0.5980,0.0122) | (0.71556, 0.1965) | (0.5794,-0.20) |

The eigenvalues show that of the two physically meaningful fixed points, (ρ_1^*, σ_1^*) is an unstable fixed point and (ρ_2^*, σ_2^*) is a saddle one. Figure 3 shows the flow of the

phase plane trajectories toward the unstable fixed point ($\rho_1^* = 0.4, \sigma_1^* = 0.01$) in the $\tilde{x} \rightarrow -\infty$ limit for various initial values. Although, one can attempt to draw the

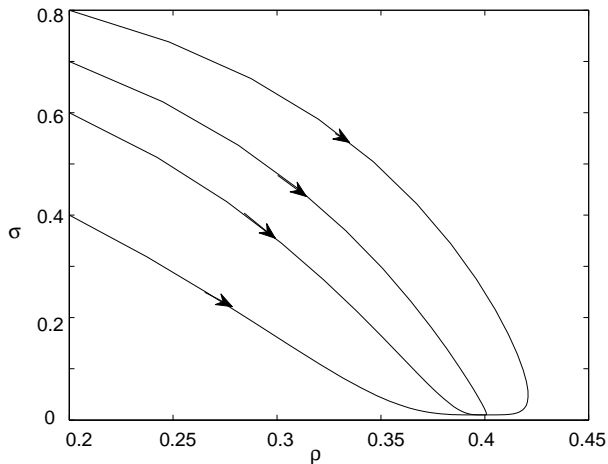


FIG. 3: Phase-plane diagram on the $\rho - \sigma$ plane for different initial conditions with $m = 0.4$. Initial conditions $(\rho(\tilde{x} = 0), \sigma(\tilde{x} = 0))$ as we move towards the outermost line are $(0.2, 0.4)$, $(0.2, 0.6)$, $(0.2, 0.7)$, $(0.2, 0.8)$. The arrows on the lines, indicate the direction of more negative values of \tilde{x} .

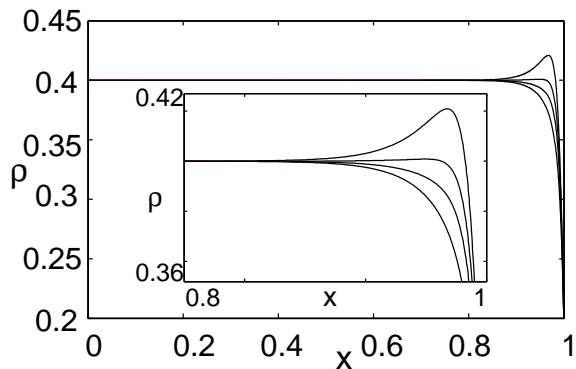


FIG. 4: Density profiles (ρ) plotted for $m = 0.4$ and left boundary conditions $(\rho_l, \sigma_l) = (0.4, 0.01)$. Right boundary conditions, here, are same as the initial conditions of figure 3. The lower most profile corresponds to $(\rho_r, \sigma_r) = (0.2, 0.4)$. The rest follow the same order as specified in figure 3. All the plots are obtained with $\epsilon = 0.006$.

flow trajectories intuitively, flow trajectories in the figures are obtained by numerically solving equations (13) and (14) with values of c_1 and d_1 determined using equations (15) and (16). Figure 3 indicates that for values of (ρ_r, σ_r) same as the initial conditions of figure 3 and for $(\rho_l = 0.4, \sigma_l = 0.01)$, the density profiles must have a boundary layer part near $x = 1$ merging to constant bulk profiles with $\rho_b = 0.4$ and $\sigma_b = 0.01$. This bulk part satisfies the boundary condition at $x = 0$. Numerical solutions of the hydrodynamic equations for these boundary conditions are shown in figures 4 and 5. Figure 3 shows that the trajectory with initial condition

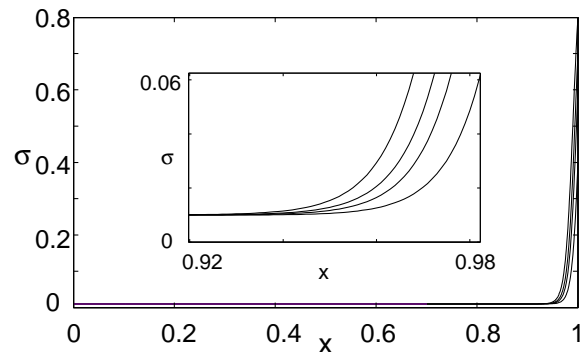


FIG. 5: Density profiles, σ , plotted for $m = 0.4$ and same boundary conditions as that of figure 4. The lower most profile corresponds to $(\rho_r, \sigma_r) = (0.2, 0.4)$. The rest follow the same order as specified in figure 3. All the plots are obtained with $\epsilon = 0.0062$.

$(\rho, \sigma) = (0.2, 0.8)$ comes to close proximity of the saddle fixed point. This is reflected in the boundary layer of the density profile plotted in figure 4 with boundary condition, $(\rho_r, \sigma_r) = (0.2, 0.8)$. We next study how a trajectory with a given initial condition changes with m . Figure 6 shows phase plane trajectories with initial condition $(0.2, 0.8)$ for different values of m . From

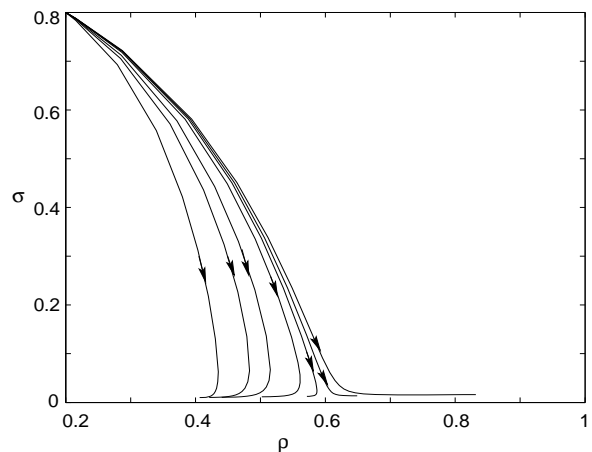


FIG. 6: Phase-plane diagram on the $\rho - \sigma$ plane for different values of m . Trajectories are drawn with initial condition $\rho(\tilde{x} = 0) = 0.2$ and $\sigma(\tilde{x} = 0) = 0.8$. The arrows indicate the direction of more negative value of \tilde{x} . Values of m for various lines as we move towards the outermost line are 0.45, 0.58, 0.64, 0.70, 0.72, 0.73 and 0.74. The flow of the trajectories changes at $m \approx 0.725$.

this figure, it appears that there exists a special value of m , say, m_c , for which the trajectory is a separatrix which approaches the saddle fixed point. Our numerical solutions show $m_c \approx .725$. Hence, for $m < m_c$ and $(\rho_r = 0.2, \sigma_r = 0.8)$, the bulk-densities are $\rho_b = 0.4$ and

$\sigma_b = 0.01$. At $m = m_c$, the bulk density value discontinuously changes to $\rho_b \approx 0.597$, $\sigma_b = 0.0125$. Naturally, now the boundary layers are present at both the boundaries to satisfy respective boundary conditions. These boundary layers are the two separatrices that approach (emerge) to (from) the saddle fixed point. Density profiles with different values of m are presented in figure 7. The inset in figure 7 shows that the boundary layer near $x = 0$ becomes sharper as the value of ϵ is reduced. The fact that,

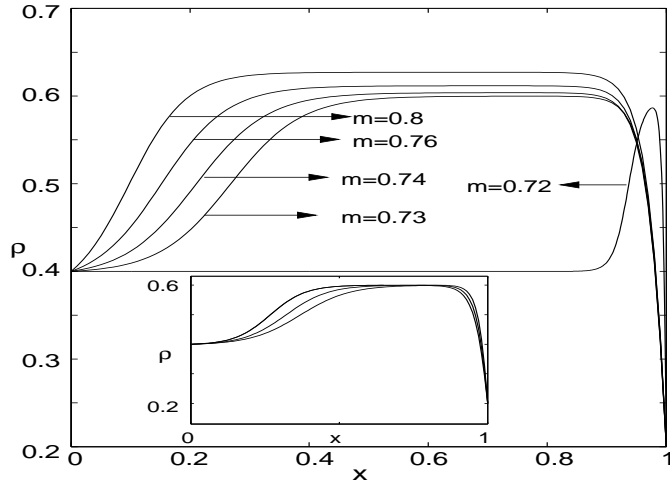


FIG. 7: Density profiles for different values of m with boundary conditions ($\rho_l = 0.4, \sigma_l = 0.01$) and ($\rho_r = 0.2, \sigma_r = 0.8$). Values of ϵ for the density profiles with $m = 0.72$ and 0.73 are $.00025$ and 0.012 , respectively. The rest of the profiles are obtained with $\epsilon = 0.0125$. Inset shows the change in the shape of the density profile for $m = 0.73$ as ϵ is changed. Values of ϵ as one moves towards the outermost curve are 0.016 , 0.014 and 0.012 .

for $m > m_c$, the bulk density continues to be described by a saddle fixed point is clear from the boundary layers at both the ends.

Boundary layers for the equations in (9) and (10) satisfy the following first order equations,

$$(1 - m\sigma) \frac{d\rho}{d\tilde{x}} = \rho(1 - \rho)(1 - m\sigma) + c_2 \quad (17)$$

$$(1 - m\rho) \frac{d\sigma}{d\tilde{x}} = \sigma(1 - \sigma)(1 - m\rho) + d_2, \quad (18)$$

where, as before, c_2 and d_2 are two integration constants. These nonlinear terms do not disturb the boundary layer fixed points and since $0 \leq m \leq 1$ and $0 \leq \rho, \sigma \leq 1$, the stability properties of the fixed points also remain the same as before. These new factors only introduce minor, quantitative changes in the flow trajectories and in the value of m_c . The flow trajectories for these differential equations with the initial condition, $(\rho, \sigma) = (0.2, 0.8)$, and different values of m are shown in figure 8. As a consequence, here also the density profiles indicate a discontinuous change in the bulk density as the value of m is increased. This result contradicts earlier results of

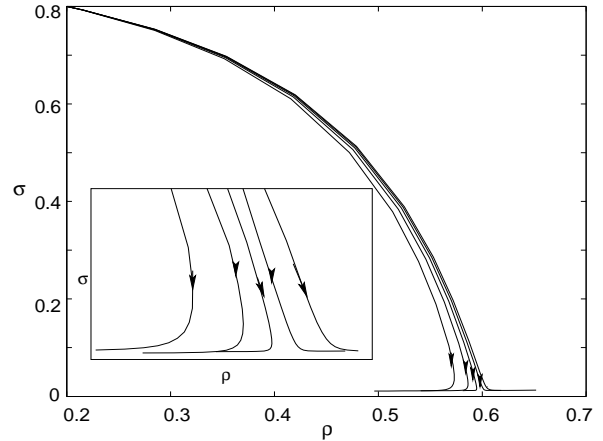


FIG. 8: Phase-plane diagram for the boundary layer equations with non-linear regularization terms. Values of m as one approaches the outermost line are $0.63, 0.64, 0.645, 0.648$ and 0.65 . Trajectories are obtained with initial conditions $\rho(\tilde{x} = 0) = 0.2$ and $\sigma(\tilde{x} = 0) = 0.8$. Arrows on the line indicate direction along which \tilde{x} becomes more negative. A zoomed version of the same figure is shown in the inset.

[8] where, from numerical solutions of the hydrodynamic equations (9) and (10), it has been concluded that increasing the value of m does not cause a sudden change in the value of the bulk density. The present analysis brings out the mathematical reason behind such a discontinuous change. Our numerical solutions of the hydrodynamic equations obtained using MATLAB appear to be consistent with this observation.

IV. MODEL-2: TWO-LANE PROCESS WITH PARTICLE EXCHANGE

Here we consider a system of two lanes with hopping of particles from one lane to the other [12, 13]. Particle dynamics on the lanes are governed by the following rules (See figure (9)). (a) On one of the lanes, say lane-E,

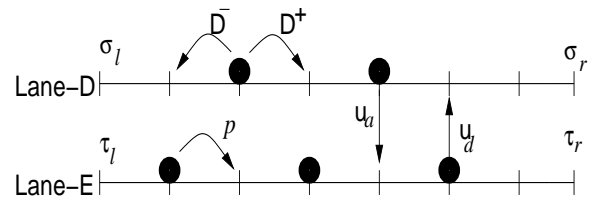


FIG. 9: Particle dynamics on the two lanes for model-2.

particles undergo asymmetric simple exclusion process. This implies that particles hop to the neighboring site in a specific direction provided it is empty. We assume the hopping rate to be p here.

(b) On the other lane, say lane-D, particles are not subjected to exclusion interaction and have biased diffusion with hopping rates to left and right being D^- and D^+ respectively.

(c) A particle at the i th site on lane-E can hop to the i th site of lane-D at rate u_d and the reverse process i.e. an attachment of a particle to lane-E from lane-D can take place at rate, u_a , provided the target site on lane-E is empty.

In the steady state, the continuum limit of the statistically averaged master equations is

$$\epsilon D_\tau \frac{\partial^2 \tau}{\partial x^2} - \frac{\partial J_\tau}{\partial x} - D\tau + A\sigma(1 - \tau) = 0, \quad (19)$$

$$\epsilon D_\sigma \frac{\partial^2 \sigma}{\partial x^2} - \frac{\partial J_\sigma}{\partial x} + D\tau - A\sigma(1 - \tau) = 0, \quad (20)$$

where $D_\tau = p/2$, $D_\sigma = (D^+ + D^-)/2$, $D = u_d N$, $A = u_a N$ and $\epsilon = 1/N$. Here $\tau(x)$ and $\sigma(x)$ are the average densities of particles on the lanes with ASEP and biased diffusion respectively with currents on these lanes being

$$J_\tau = p\tau(1 - \tau), \quad \text{and} \quad J_\sigma = v\sigma. \quad (21)$$

Here, $v = D^+ - D^-$ denotes the net average velocity of particles along lane-D. In addition, we assume that the particle reservoirs impose the boundary conditions ($\tau(x=0) = \tau_l, \sigma(x=0) = \sigma_l$) and ($\tau(x=1) = \tau_r, \sigma(x=1) = \sigma_r$).

Constant bulk profiles are expected if the terms due to particle exchange between the lanes disappear altogether [12, 13]. This happens under the condition

$$\sigma = \frac{D}{A} \frac{\tau}{1 - \tau}. \quad (22)$$

In the following subsection, we consider this model of constant bulk profile. Although the phase-diagram for the constant profile case has been obtained earlier [13], this analysis allows us to see how the maximal and minimal current phases and upward and downward shocks appear naturally due to the flow of the boundary layer solution toward specific fixed points. This study also provides an ideal platform to compare this case with that of a non-constant bulk profile considered in the next subsection. Therefore, apart from examples with different boundary conditions, the next subsection, also contains a part in which major differences from the constant bulk profile case are discussed.

A. Constant bulk profile

Adding equations (19) and (20), and using (22), we obtain the following steady state equation for τ

$$\epsilon \frac{\partial}{\partial x} \left[D_\tau \frac{\partial \tau}{\partial x} + D_\sigma D_{\text{ad}} \frac{\partial}{\partial x} \left(\frac{\tau}{1 - \tau} \right) \right] - \frac{\partial}{\partial x} \left[v D_{\text{ad}} \frac{\tau}{1 - \tau} + p\tau(1 - \tau) \right] = 0, \quad (23)$$

which should be solved in the presence of the boundary conditions, $\tau(x=0) = \tau_l$ and $\tau(x=1) = \tau_r$. Here, $D_{\text{ad}} = D/A$. Terms within the second square bracket of equation (23) together give the total current $J_{\text{tot}} = J_\tau + J_\sigma$ on the two lanes. Special values of τ , τ_M and τ_m , corresponding to maximum and minimum of J_{tot} (see figure 10) play an important role in the phase-plane analysis.

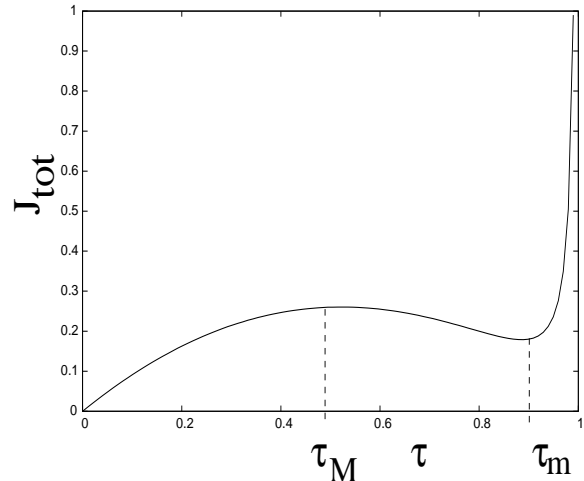


FIG. 10: J_{tot} is plotted with τ . For this plot, $v = p = 1$ and $D_{\text{ad}} = 0.01$.

Once again, the boundary layers are the solutions of the second order differential equation (23) which after one integration appears as

$$\frac{\partial \tau}{\partial \tilde{x}} \left[D_\tau + D_\sigma D_{\text{ad}} \frac{1}{(1 - \tau)^2} \right] - \left[v D_{\text{ad}} \frac{\tau}{1 - \tau} + p\tau(1 - \tau) \right] = c, \quad (24)$$

Here c is the integration constant and $\tilde{x} = \frac{x - x_0}{\epsilon}$. Saturation of the boundary layer to the bulk density, τ_b , requires

$$c = -v D_{\text{ad}} \frac{\tau_b}{1 - \tau_b} - p\tau_b(1 - \tau_b). \quad (25)$$

Since $0 \leq \tau_b \leq 1$, the value of c lies in the range $-\infty < c < 0$. For a single differential equation as (24), one can have a two-dimensional fixed point diagram as shown in figure 11. This is an additional advantage of the present system over the previous one.

The basic principle for finding the density profiles using the fixed point diagram is that the shocks or the boundary layers in the profiles correspond to vertical straight lines on the fixed point diagram moving from one fixed point branch to the other following the stability properties. For example, an upward shock in the bulk of the density profile may connect a low-density at the lower fixed point branch to a higher density in the middle fixed point branch.

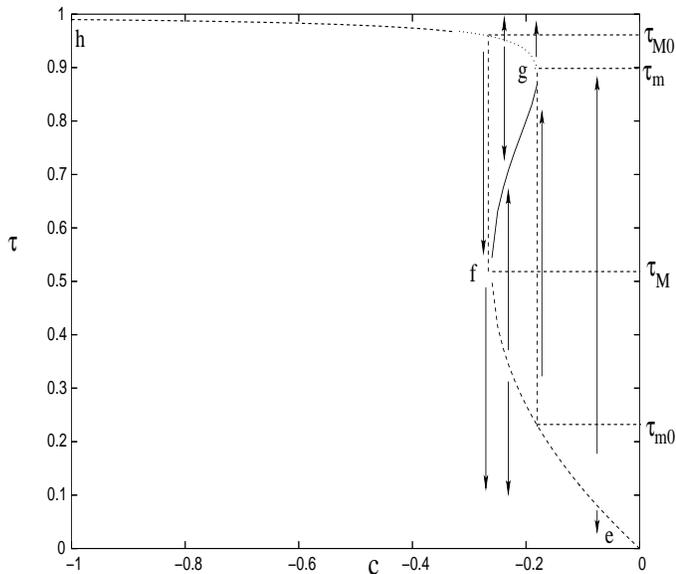


FIG. 11: Fixed point diagram on the $c - \tau$ plane for the parameter values $v = 1$, $p = 1$ and $D_{\text{ad}} = 0.01$. The arrowed vertical lines show the stability properties of various fixed point branches. Three fixed point branches, ef, fg and gh are referred in the text as lower, middle and upper branch respectively.

(a) Given this rule, the density profile can have localized shocks under the following conditions. (i) $\tau_{m0} < \tau_l < \tau_M$, $\tau_M < \tau_r < \tau_m$ and $c(\tau_l) = c(\tau_r)$.

Pictorially, an upward shock is possible if τ_l located in the lower fixed point branch can be connected to τ_r in the middle branch through only a vertical straight line. This constraint is stated mathematically through the above equality satisfied by c . Let us assume that for a given τ_r in the middle branch, the localized shock appears if $\tau_l = \tau_{lc}$ (See figure 12.). Now for $\tau_l = \tau_{l1} < \tau_{lc}$, the flow behavior allows a density profile with a bulk part satisfying the boundary condition at $x = 0$ and a boundary layer near $x = 1$. This kind of boundary layer is represented by vertical line (1) in figure 12. In this case, it is not possible to have a boundary layer at $x = 0$ since that would imply a vertical line passing through τ_l and going further upward after crossing τ_r . Although such a line passes through both τ_l and τ_r , it cannot represent a bulk profile. Similarly, for $\tau_l = \tau_{l2} > \tau_{lc}$, a profile, with bulk satisfying the boundary condition at $x = 1$ and a boundary layer near $x = 0$ represented by line (2) in figure 12, is the only solution.

(ii) A downward shock in the bulk profile can be present when $\tau_m < \tau_l < \tau_{M0}$ and $\tau_M < \tau_r < \tau_m$ and $c(\tau_l) = c(\tau_r)$. In this case, a bulk profile of value τ_l at left is joined to a bulk density of value τ_r through a downward shock.

(iii) Another very special line on which localized upward shocks can be present is given by $\tau_r > \tau_m$ and

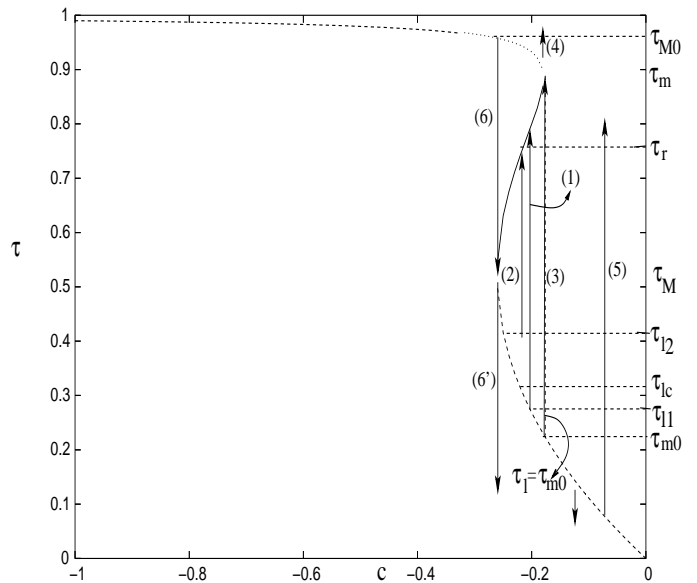


FIG. 12: Fixed point diagram of figure 11. Vertical lines are numbered in order to refer these in the text in the context of different boundary layers and shocks.

$\tau_l = \tau_{m0}$. The shock here joins τ_l to the minimum current density τ_m . The density profile at $x = 0$ starts with a constant value τ_l and then reaches another constant part τ_m through a shock, represented by the vertical line (3) in figure 12, and finally satisfies the boundary condition τ_r through a boundary layer, represented by the vertical line (4) in the figure.

Approach of a shock or a boundary layer to the bulk density is governed by equation (24). The variation of a small perturbation $\delta\tau$ near the saturation to a bulk density τ_b is given by

$$\frac{d\delta\tau}{dx} f(\tau_b) = \left[\frac{vD_{\text{ad}}}{(1-\tau_b)^2} + p(1-2\tau_b) \right] \delta\tau, \quad (26)$$

where $f(\tau) = D_\tau + D_\sigma D_{\text{ad}} \frac{1}{(1-\tau)^2}$. Thus the approach of a boundary layer to the bulk is in general exponential except at special bulk values $\tau_b = \tau_m, \tau_M$. The length scale associated with the exponential approach to the bulk diverges at these special values [13, 15].

(b) Boundary conditions for which a minimal current phase may appear: The flow lines clearly show that for $\tau_r > \tau_m$ and $\tau_{m0} < \tau_l < \tau_m$, a shock connecting τ_l to the middle branch is not helpful for meeting the boundary condition at $x = 1$. In this case the only option is to have a boundary layer at $x = 0$ connecting τ_l to τ_m and then a constant bulk profile of density τ_m followed by a boundary layer at $x = 1$. Such a boundary layer must be represented by line (3) in figure 12. Note that this is the only possibility since any other parallel vertical line with $c > c(\tau_m)$ will correspond to an unphysical solution. This explains how a minimal current density profile becomes an obvious solution for boundary densities in this region.

For the opposite case, $\tau_l < \tau_{m0}$ and same τ_r , the density should have a constant value τ_l with a boundary layer at $x = 1$ represented by line (5) in figure 12.

(c) Boundary conditions for which a maximal current phase may appear: For $\tau_M < \tau_l < \tau_{M0}$ and $\tau_r < \tau_M$, the only possibility is to have a boundary layer at $x = 0$ represented by line (6) in figure 12. This line meets the fixed point curve at τ_M which continues as the bulk density. The boundary condition at $x = 1$ is met by another downward vertical line (6'). It is clear that if $\tau_l = \tau_{M0}$, the density profile can have a localized downward shock of height $\tau_{M0} - \tau_M$. The bulk density will no longer have a value τ_M if $\tau_l > \tau_{M0}$. In that case, the only possible shape for the density profile is a flat profile of density τ_l followed by a downward boundary layer satisfying the boundary condition τ_r .

B. Non-constant bulk profile

In this section, we illustrate how a similar analysis as that of the previous sub-section can be extended to a case of a non-constant bulk profile. In order to produce a non-constant bulk profile, we artificially add a term to equation (23). This kind of term has appeared earlier in the steady-state equation ASEP with Langmuir kinetics [16]. However, for this model, this term only has a mathematical implication of producing a non-constant bulk profile. The final steady state equation for the density τ is

$$\epsilon \frac{\partial}{\partial x} \left[D_\tau \frac{\partial \tau}{\partial x} + D_\sigma D_{ad} \frac{\partial}{\partial x} \left(\frac{\tau}{1-\tau} \right) \right] - \frac{\partial}{\partial x} \left[v D_{ad} \frac{\tau}{1-\tau} \right] + p\tau(1-\tau) + \Omega(1-2\tau) = 0. \quad (27)$$

Ignoring the second order derivative term in (23), one may consider a simplified equation, valid at $O(\epsilon^0)$, as

$$\left[\frac{v D_{ad}}{(1-\tau)^2} + p(1-2\tau) \right] \frac{\partial \tau}{\partial x} + \Omega(2\tau - 1) = 0. \quad (28)$$

As mentioned earlier, the solution of this equation describes the bulk profile. In principle, one can solve this equation explicitly to find the bulk parts of the density profile. However, as we shall show, the shape of the profile can be predicted without explicitly solving this or the boundary layer equation.

After a brief comparison between the two cases with constant and non-constant bulk profiles, we discuss a few examples with different boundary conditions. To show that our approach gives the right profile, we illustrate these examples with typical density profiles obtained by solving the hydrodynamic equation numerically. We hope that these ideas can be implemented more generally for all other boundary conditions that are not discussed here.

Comparison between the cases with constant and non-constant bulk profiles:

The major difference from the previous analysis is that for a flat bulk profile, there is no variation in the density, once the boundary layer merges to a fixed point. The density in the bulk remains constant at this fixed point value. This need not be the case here and, in general, the density varies along various fixed point branches after the boundary layer merges to a fixed point. Thus the entire density profile can be predicted, by knowing only the slope of the density profile in the bulk and following the vertical arrowed lines for the boundary layer parts. The slope of the bulk profile can be determined from (28) and the arrows on the fixed point branches in figure 13 represent increasing or decreasing nature of the bulk density with x . Since for a flat profile, the density at the bulk has to remain constant at τ_l , τ_r or at very special values like, say, τ_M , the possibility of seeing localized shock here is restricted. The shock appears only when these values are such that they can be connected through vertical lines in the interior of a lane. Such limitations are not present here since the varying bulk density may reach certain values which can be connected by vertical lines in the bulk. It is because of this that seeing localized shocks over a region in the phase diagram becomes more likely, in general, whenever the bulk density is not constant and its slope is appropriate for supporting a shock. Such a phase diagram with a wide region of localized shock was reported initially in [16].

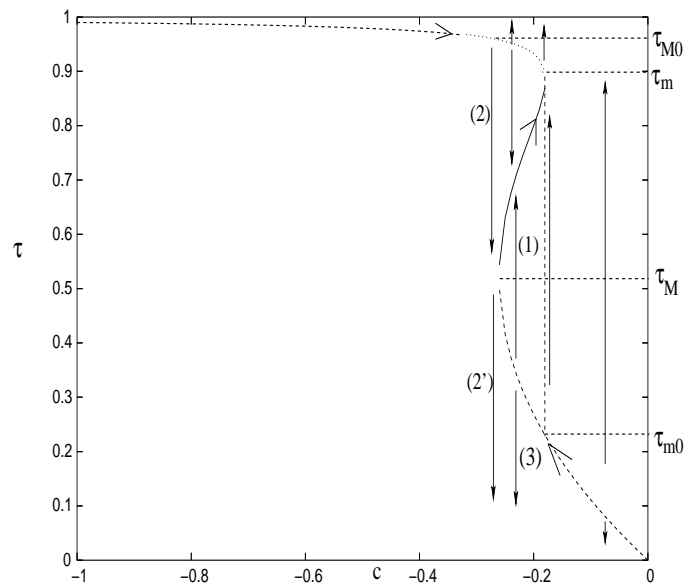


FIG. 13: Fixed point diagram of figure 11. Vertical lines are numbered in order to refer these in the text in the context of different shocks and boundary layers.

$$\tau_l < \tau_{m0} \text{ and } \tau_M < \tau_r < \tau_m :$$

There cannot be a boundary layer at $x = 0$ since that would correspond to a vertical flow line passing through

τ_l and the density profile will not correspond to a physically meaningful solution. However, a bulk profile satisfying the boundary condition at $x = 0$ is possible. This is an increasing profile along the lower fixed point branch. From this lower branch, there are two ways to satisfy the boundary condition at $x = 1$: (a) through a shock (represented by a vertical line in the phase plane) connecting the low-density bulk part in the lower branch to a high-density bulk part in the middle branch. This latter bulk part, with a positive slope (see the upward arrow along the middle fixed point branch) finally satisfies the boundary condition at $x = 1$. (b) through a boundary layer (represented by a vertical line in the phase plane) that connects the bulk density in the lower branch to a density in the middle branch. The boundary layer satisfies the boundary condition at $x = 1$ before it saturates to the other fixed point. Figure 14 shows a density profile following option (b).

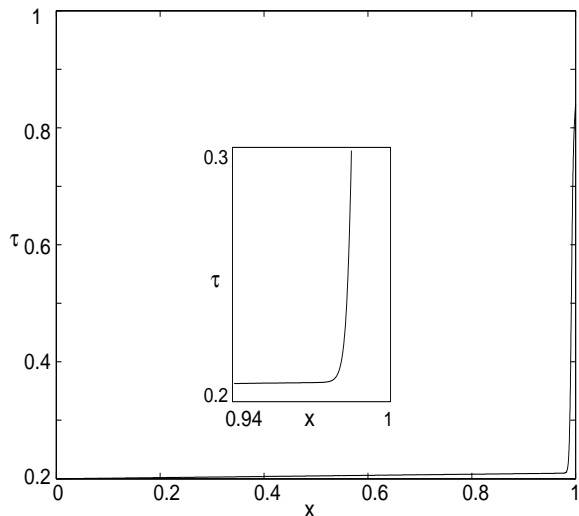


FIG. 14: Density profile for $\tau_l = 0.2$ and $\tau_r = 0.84$. Values of other parameters are $\epsilon = 0.002$, $v = p = 1$, $D_{ad} = 0.01$, $\Omega = 0.01$ and $D_\sigma = 1$.

$$\tau_{m0} < \tau_l < \tau_M \text{ and } \tau_M < \tau_r < \tau_m:$$

An increasing bulk density satisfying the boundary condition at $x = 0$ may be connected to another bulk part in the middle branch through a shock represented by the vertical line (1) in figure 13. This is similar to option (a) of the previous example. Such a density profile appears as shown in figure 15. There are still two other options each with an upward boundary layer. One possibility is that an upward boundary layer at $x = 0$ meets the middle fixed point branch and a bulk part continuing from there finally satisfies the boundary condition at $x = 1$. The other possibility is that a bulk part with positive slope satisfies the boundary condition at $x = 0$ and

an upward boundary layer following the bulk satisfies the boundary condition at $x = 1$.

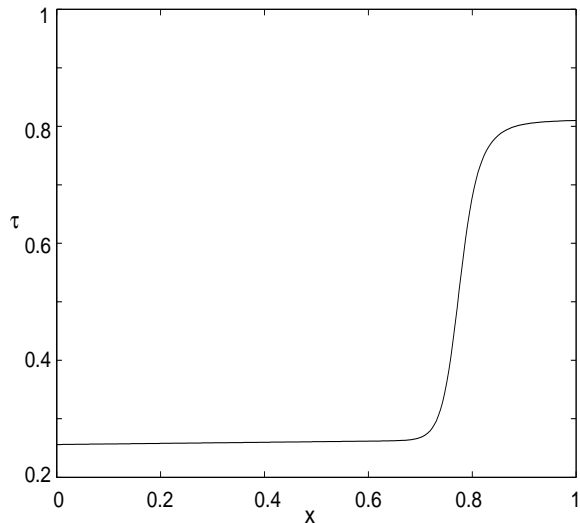


FIG. 15: Density profile with a shock for $\tau_l = 0.256$, $\tau_r = 0.81$ and $\epsilon = 0.015$. Values of other parameters are same as those of figure 14

$$\tau_r < \tau_M \text{ and } \tau_M < \tau_l < \tau_m:$$

This is a very unique situation for the following reasons. Figure 13 shows that there is only one route on the fixed point diagram that the density profile must follow to satisfy both the boundary conditions. At $x = 0$, there must be a boundary layer of negative slope (represented by a vertical line (2)) merging to density τ_M . This should be followed by another downward profile (represented by (2')) that satisfies the boundary condition at $x = 1$. The entire density profile is thus described by only two vertical lines (2) and (2'). A 'bulk' like part of almost constant value ($\approx \tau_M$) does appear in the density profile (see figure 16). However, this is not a real bulk profile since τ_M is not a solution of (28). It looks like a bulk density since the slopes of the vertical lines (2) and (2') vanish at $\tau = \tau_M$ and hence the profile looks almost flat. $\tau = \tau_M$ is in fact a point of inflection of the density profile. In this sense, there is a subtle difference between the maximal current phase seen here and in the simple ASEP model for which the bulk-density value, $1/2$, is a solution of the corresponding outer equation [19].

$$\tau_l, \tau_r < \tau_{m0} \text{ and } \tau_l > \tau_r:$$

The bulk profile must satisfy the boundary condition at $x = 0$ and increase along the lower branch and then satisfy the other boundary condition through a boundary layer of negative slope at $x = 1$, represented by a vertical line (3) in the figure 13. A typical density profile appears as shown in figure 17.

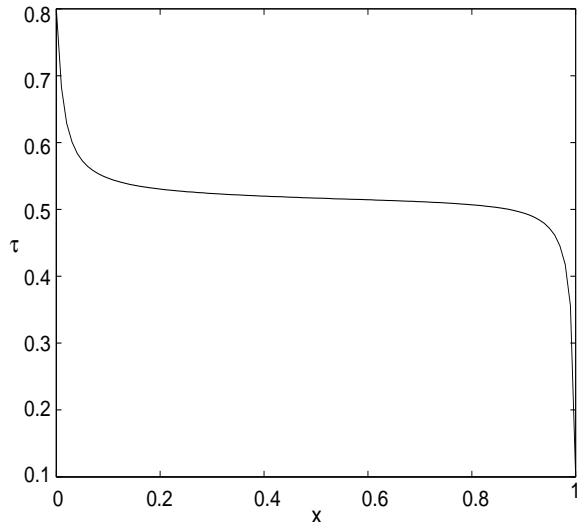


FIG. 16: Density profile for $\tau_l = 0.8$, $\tau_r = 0.1$ and $\epsilon = 0.005$. Values of other parameters are same as those of figure 14.

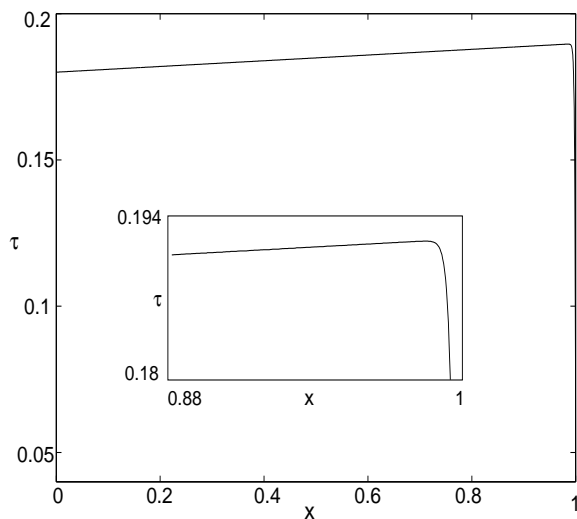


FIG. 17: Density profile for $\tau_l = 0.18$, $\tau_r = 0.04$ and $\epsilon = 0.002$. Values of other parameters are same as those of figure 14.

V. CONCLUSION

We have shown how the phase-plane behavior of the boundary-layer equation can be used to understand the shape of the steady-state density profile of multi-lane driven exclusion processes. We have considered two distinct multi-lane processes. In the first model, the lanes do not exchange particles but the particle dynamics on the two lanes are coupled since hopping of particles on one

lane is affected by the particle occupancies on the neighboring lane. In the hydrodynamic approach, the boundary layers of the density profiles on the two lanes are described by coupled nonlinear equations. Using phase plane trajectories, we show that, as the interaction between the lanes is increased, the bulk density, for certain boundary conditions, may increase discontinuously due to the influence of a saddle fixed point. This has been done using linear phenomenological regularization terms for the differential equations. Since this method does not require explicit solution of the density profile, it can be easily extended to other system of equations with nonlinear regularizing terms. One such case with nonlinear regularizing terms has been discussed here. The second model involves two lanes which can mutually exchange particles. In addition, particles in one lane go through a driven exclusion process and those on the other lane have biased diffusion without any exclusion constraint. We consider two variants of this model; one with a constant bulk density profile and another with a non-constant bulk profile. The fixed point diagram shows saddle node bifurcations of the fixed points of the boundary-layer equation. For constant bulk profile, the fixed point diagram allows us to predict the density profiles and the location of the boundary layers uniquely under various boundary conditions. For non-constant bulk-profile, one requires an additional information regarding the slope of the bulk solution. Some of the useful features of the method are as follows. With the required information about the bulk profile, one can exactly predict under which condition boundary layer or shock will have positive or negative slope. Similar analysis can be done with ease for different parameter values which may reverse the slopes of the bulk solutions on some of the fixed point branches or change the fixed-point diagram significantly. Analysing the two cases of constant and non-constant profiles, it becomes transparent as why localized shocks appear only under restricted boundary conditions for a flat profile but over a wide range of boundary conditions for a non-constant profile.

We have analysed the first model for only some specific boundary conditions and we have not made any attempt to explore the phase diagram although the method can be used in a similar manner for other boundary conditions also. There are several aspects which may make the analysis interesting. One, for example, is the presence of more number of physically acceptable fixed points. This, apart from leading to interesting phase portraits, may reveal the role of various eigenvalues in deciding the shape of the density profile. Second, is the presence of imaginary eigenvalues which may be responsible for oscillatory density profiles. Whether the multi-lane problem considered here has this kind of complexity can be explored through a detailed analysis for the full phase-diagram. This work is in progress.

For the second model, the condition relating the two densities on the two lanes simplifies the problem in two ways. First, it leads to constant density profile and sec-

ond, due to this relation, it becomes sufficient to consider hydrodynamic equation for a single density variable. In the absence of such a condition, individual boundary layer equations look apparently decoupled at the lowest

order. The boundary layer analysis for the two densities would, however, be coupled due to the coupled nature of the bulk equations. This may give rise to an interesting boundary layer analysis not encountered earlier.

-
- [1] Krug J, 1991 *Phys. Rev. Lett.* **67** 1882
 - [2] Evans M R, Foster D P, Godreche C and Mukamel D, 1995 *Phys. Rev. Lett.* **74**, 208; 1995 *J. Stat. Phys.* **80** 69
 - [3] Janowsky S A and Lebowitz J L, 1992 *Phys. Rev. A* **45** 612
 - [4] Mukamel D., 2000 *Soft and Fragile Matter: Nonequilibrium Dynamics, Metastability and Flow* (Bristol: IoP publishing)
 - [5] Derrida B, Domany E and Mukamel D, 1992 *J. Stat. Phys.* **69** 667
 - [6] Popkov V, 2007 *J. Stat. Mech.* P07003; Popkov V and Schütz G M, *J. Stat. Mech.* P12004
 - [7] Mukherji S, 2009 *Phys. Rev. E* **79** 041140
 - [8] Popkov V and Schütz, 2003 *J. Stat. Phys.* **112** 523 (2003); Popkov V and Salerno M, (2004) *Phys. Rev. E* **69** 046103
 - [9] Popkov V and Peschel I, 2001 *Phys. Rev. E* **64**, 026126
 - [10] Klumpp S and Lipowsky R, 2003 *J. Stat. Phys.* **113**, 233
 - [11] Harris R J and Stinchcombe R B, (2005) *Physica A* **354**, 582
 - [12] Tailleur J, Evans M R, and Kafri Y, 2009 *Phys. Rev. Lett.* **102** 118109
 - [13] Evans M R, Kafri Y, Sugden K E P and Tailleur J, 2011 *J. Stat. Mech.* P06009
 - [14] Melbinger A, Reichenbach T, Franosch T and Frey E, (2011) *Phys. Rev. E* **83** 031923
 - [15] Hager J S, Krug J, Popkov V and Schütz G M, 2001 *Phys. Rev. E* **63** 056110; Popkov V, Rákos A, Willmann R D, Kolomeisky A B and Schütz G M, 2003 *Phys. Rev. E* **67** 066117
 - [16] Parameggiani A, Franosch T and Frey E, 2004 *Phys. Rev. E* **70** 046101; Evans M R, Juhász R and Santen L, 2003 *Phys. Rev. E* **68** 026117
 - [17] Mukherji S and Bhattacharjee S M, 2005 *J. Phys. A* **38** L285; S. Mukherji and V. Mishra, 2006 *Phys. Rev. E* **74** 01116
 - [18] Bhattacharjee SM in *Continuous models and discrete systems*, edited by Jeulin D and Forest S (Ecole des mine, Paris, 2008)
 - [19] Bhattacharjee S M, 2007 *J. Phys. A* **40** 1703
 - [20] Cole J D, 1968 *Perturbation Methods in Applied Mathematics* (Massachusetts: Blaisdell Publishing)
 - [21] Popkov V and Schütz G M, 1999 *Euro. Phys. Lett.* **48** 257
 - [22] Strogatz S H, *Nonlinear dynamics and chaos* (Perseus Books, Cambridge, 1994)